

**vuv fluorescence from selective high-order multiphoton excitation of N<sub>2</sub>**

Ryan N. Coffee\* and George N. Gibson

*Department of Physics, University of Connecticut, Storrs, Connecticut 06269, USA*

(Received 11 September 2003; published 12 May 2004)

Recent fluorescence studies suggest that ultrashort pulse laser excitation may be highly selective. Selective high-intensity laser excitation holds important consequences for the physics of multiphoton processes. To establish the extent of this selectivity, we performed a detailed comparative study of the vacuum ultraviolet fluorescence resulting from the interaction of N<sub>2</sub> and Ar with high-intensity infrared ultrashort laser pulses. Both N<sub>2</sub> and Ar reveal two classes of transitions, inner-valence  $ns \leftarrow np$  and Rydberg  $np \leftarrow n'\ell'$ . From their pressure dependence, we associate each transition with either plasma or direct laser excitation. Furthermore, we qualitatively confirm such associations with the time dependence of the fluorescence signal. Remarkably, only N<sub>2</sub> presents evidence of direct laser excitation. This direct excitation produces ionic nitrogen fragments with inner-valence ( $2s$ ) holes, two unidentified transitions, and one molecular transition, the  $N_2^+ : X \ ^2\Sigma_g^+ \leftarrow C \ ^2\Sigma_u^+$ . We discuss these results in the light of a recently proposed model for multiphoton excitation.

DOI: 10.1103/PhysRevA.69.053407

PACS number(s): 33.80.Rv, 32.80.Rm, 33.20.Ni, 32.50.+d

**I. INTRODUCTION**

It has been well established that multiphoton ionization leads to direct excitation in molecules. Experiments based on ion time-of-flight spectroscopy show that molecular excitations produced by ultrafast pulses exhibit strong charge-asymmetric dissociation channels [1–3]. Furthermore, these dissociation fragments can themselves be highly excited [4,5]. However, time-of-flight spectroscopy is insensitive to the internal state of the detected ion, and so it has been difficult to identify excited fragment states. State identification is crucial for developing a detailed theory of the strong-field interaction that leads to fragment excitations.

In contrast to ion time-of-flight spectroscopy, fluorescence spectroscopy provides precise information about both the upper and lower states of observed transitions. This makes it a powerful tool for examining excited states; specifically for distinguishing inner-valence transitions,  $ns \leftarrow np$ , from Rydberg transitions,  $np \leftarrow n'\ell'$ . A major drawback however is that standard methods of vuv fluorescence detection are quite inefficient and therefore require high target gas densities. High densities in turn lead to unwanted plasma effects that complicate the spectra. Nevertheless, two previous studies of vuv radiation from the strong-field ionization of N<sub>2</sub> have identified transitions resulting from direct laser excitation [6,7]. However, neither experiment had enough dynamic range or wavelength coverage to draw firm conclusions regarding excitation selectivity.

In this paper, we present vuv fluorescence spectra generated by the interaction of high-intensity laser radiation with both N<sub>2</sub> and Ar. Using a vuv collection optic we have dramatically increased the sensitivity of our detection system relative to the previous experiments [6,7]. High dynamic range in pressure allows us to distinguish fluorescence produced by direct laser excitation from that produced by plasma excitation. Analyzing a large number of transitions in

both N<sub>2</sub> and Ar leads to several striking conclusions. First, numerous nitrogen fluorescence lines result from the direct laser production of excited photodissociation fragments. These fragments *exclusively* undergo inner-valence transitions,  $2s \leftarrow 2p$ . Second, direct laser excitation also produces two unidentified transitions and the  $N_2^+ : X \leftarrow C$  transition. Third, there is *no* evidence for direct excitation in argon. Fourth, plasma excitation is indiscriminate, producing both inner-valence and Rydberg transitions in nitrogen and argon.

High selectivity for inner-valence transitions contrasts sharply with all other excitation mechanisms in nitrogen. As the primary component of our atmosphere, N<sub>2</sub> has been extensively studied through a variety of means including plasma discharge [8], electron impact [9], extreme ultraviolet synchrotron irradiation [10], and x-ray ionization [11]. None of these experiments show the excitation selectivity observed in our present work. It is precisely this selectivity that allows us to speculate on the mechanism for the strong-field excitation. In particular, we consider three models for excitation: laser-induced resonance [12], laser-induced electron rescattering [13], and a recently proposed theory of highly efficient multiphoton coupling in diatomic molecules [14,15].

It has been known for many years that strong laser fields produce large ac Stark shifts in atoms and molecules [12]. As the laser intensity varies throughout the pulse duration, states can shift briefly into multiphoton resonance and mediate ionization. This leads to peaks in the photoelectron spectrum—the so-called “Freeman” resonances [16]. Furthermore, small populations may survive ionization and remain in the excited states. Since we would expect a remaining  $\sim 1\%$  excitation in argon [17], any direct argon fluorescence is a measure of laser-induced resonance. However, direct fluorescence in argon lies below our detection threshold while our strongest direct fluorescence in nitrogen is over three orders of magnitude above that threshold. Whatever the mechanism, the excitation presented here is vastly more efficient than laser-induced resonance.

Another possibility for excitation is the inelastic rescattering of electrons from the ion core [13]. Electrons driven by the ionizing field may return to the parent ion where they can

\*Email address: coffee@phys.uconn.edu

produce electronic excitation [18]. However, rescattering phenomena are absent in a circularly polarized field since the electron will never return to the parent core [19,20]. Since all fluorescences tested are observed with both linear and circular polarization, we rule out rescattering as the excitation mechanism.

More recently, a model has been proposed for high multiphoton susceptibility in diatomic molecules. It is well known that diatomic molecules possess a class of states called charge-transfer states [21]. Degenerate in homonuclear molecules at large internuclear separation, these states may be quite susceptible to high-order ( $n > 10$ ) multiphoton excitation [14,15]. In  $N_2^{4+}$  for instance, a pair of charge-transfer states is composed of the  $2\sigma_g$  and  $2\sigma_u$  molecular orbitals [22]. Beyond leading to asymmetric dissociation, these orbitals also primarily correlate with the fragment  $2s$  atomic state [23]. Dissociation with a persistent  $2\sigma^{-1}$  excitation would produce at least one fragment with a  $2s$  hole. This scenario is consistent with our observations: (1) we observe fluorescence from *exclusively*  $2s^{-1(2)}$  excited states in nitrogen fragments and (2) we see *no* direct fluorescence from argon—there is no atomic equivalent of charge-transfer states.

The observation of strong selective excitation by intense laser pulses suggests a range of important applications. For instance, such excitation could provide an amplification system for high harmonics and attosecond pulses. It also promises new research for high-order multiphoton transitions in molecular systems.

## II. EXPERIMENT

The laser used throughout these studies is an ultrashort pulse Ti:sapphire oscillator with an eight-pass chirped pulse amplifier [24]. The output of the laser system is 250  $\mu$ J pulses at 1 kHz repetition rate [see Fig. 1(a)]. We have a central wavelength of 800 nm and a pulse duration of  $\sim 65$  fs. The beam is focused with a 7.62 cm focal length silver mirror to a 45  $\mu$ m diameter spot. This gives a peak laser intensity near  $10^{14}$  W/cm<sup>2</sup>. As shown in Fig. 1(b), the vertical focal volume is imaged with an iridium coated, 5.08 cm focal length, spherical mirror such that the image lies along the monochromometer entrance slit. The iridium mirror has a reflectance of  $R \approx 0.20$  at normal incidence [25], and with a numerical aperture of  $F/1.33$  it collects  $\Delta\Omega/4\pi \approx 0.028$  solid angle. With this collection scheme we achieve  $\approx 0.2$  nm resolution and yet maintain an appreciable signal over the pressure range 0.05–140 mtorr. The absolute wavelength calibration is better than 0.1 nm.

Our high photon collection efficiency allows us to perform line specific pressure, time, and polarization dependence studies. We detect single vuv photons with a photomultiplier tube at the exit slit of the monochromometer. Counts registered with a leading edge discriminator then trigger a time-to-digital converter for time correlated photon counting.

We integrate photon counts over a 200 ns range to obtain signal for spectral scans and pressure dependences. We obtain over two orders of magnitude in signal dynamic range

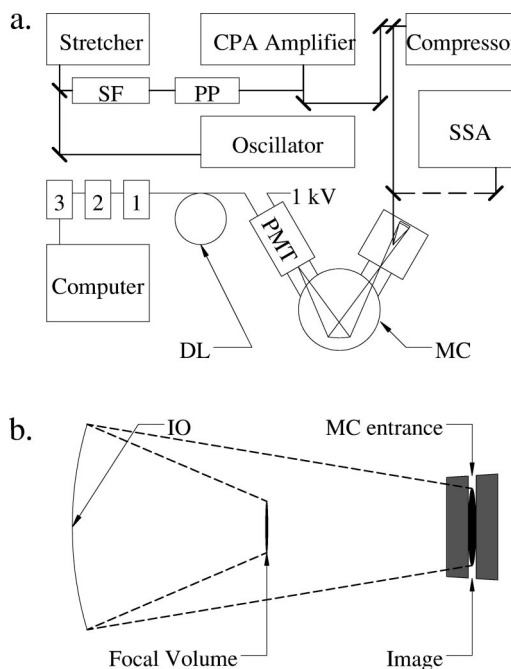


FIG. 1. (a) Schematic of the laser system: 1, fast preamplifier; 2, timing discriminator; 3, time-to-digital converter; SF, spatial filter; PP, pulse picker; SSA, single-shot autocorrelator; DL, 900 ns delay line; PMT, photomultiplier tube; and MC, monochromometer. (b). Illustration of the focal volume and its image at the spectrometer entrance slit; IO, iridium imaging optic.

for the spectra and over three orders for pressure dependence. This allows us to measure the pressure dependence for each individual fluorescence transition.

To better understand the timing data, we must investigate the impulse response of our detection scheme. In the photomultiplier assembly, vuv photons induce a sodium salicylate coated window to fluoresce at  $\sim 400$  nm [26]. This fluorescence then strikes the photocathode to produce the detection signal. In order to measure the detector response to 400 nm light (Fig. 2), we send frequency-doubled pulses directly into the monochromometer entrance slit. Modeling the impulse response with the function

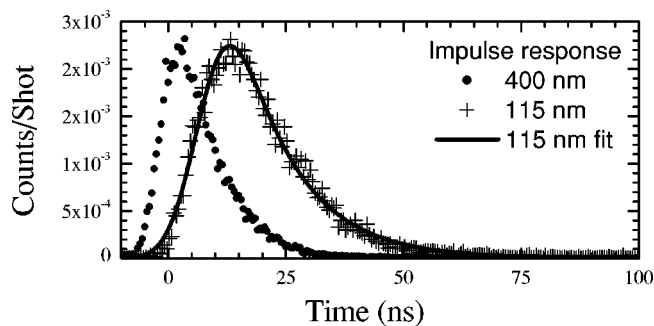


FIG. 2. (●) 400 nm impulse response of our detection scheme, (+) vuv impulse response with a fall time of 12.4 ns. Also shown is our model function [Eq. (1)] discussed in the text.

$$S_{\lambda}(t) = A \left[ \operatorname{erf} \left( \frac{t - t_{0,\lambda}}{\tau_{r,\lambda}} \right) + 1 \right] \exp \left( -\frac{t - t_{0,\lambda}}{\tau_{f,\lambda}} \right), \quad (1)$$

we can then remove any electronic and cable delay by measuring all timing with respect to  $t_{0,400}$ . Next we generate the seventh harmonic of our laser, 115 nm, and send it directly into the monochromometer as well. This allows us to characterize the fluorescence of the sodium salicylate in Fig. 2 also with Eq. (1), giving  $t_{0,115} = 9.6$  ns,  $\tau_{r,115} = 7.5$  ns, and  $\tau_{f,115} = 12.3$  ns.

Most of this study focuses on linear polarization. However, to investigate possible dependence on laser polarization, a number of representative fluorescence lines were measured with circularly polarized pulses.

### III. RESULTS

As one can see in Fig. 3, we observe many vuv fluorescence lines in both nitrogen and argon. In Table I, we list spectroscopic identifications based on the database provided by the National Institute for Standards and Technology (NIST) [27], limited to lines with observed relative intensities. The molecular identification is based on the  $N_2$  spectra compiled by Lofthus and Krupenie [8].

As mentioned above, the main challenge for vuv fluorescence spectroscopy lies in distinguishing direct laser excitation from plasma excitation. To accomplish this, we investigate the pressure dependence of each of our 18 nitrogen lines ( $a-r$ ) and seven argon lines (1–7). Direct laser excitation involves only one particle interacting with the laser field while plasma is an inherently many-body interaction. We assume the relation  $S(p) = Ap^m$ , where  $m$  is equal to the number of interacting particles needed to produce the excitation;  $m$  can then be used to differentiate direct fluorescence from plasma-induced fluorescence. By performing a linear fit to  $\ln S$  vs  $\ln p$  we equally weight high- and low-pressure data points and obtain  $m$  from the slope. Figure 4 shows such a fit for two fluorescence lines each in nitrogen and in argon. We note that this figure introduces a symbol convention that holds throughout the paper: ( $\odot$ ) inner-valence transition, ( $\bullet$ ) Rydberg transition, ( $\diamond$ )  $N_2^+ : X \leftarrow C$  transition, and ( $\times$ ) spectroscopically identified.

Direct laser excitation and plasma excitation also may evolve differently in time, providing a consistency check for pressure based determinations. We investigate this by recording the time at which photons are detected for some of our stronger lines. Unfortunately the transition rates are comparable to our impulse response and therefore we are unable to directly measure excited state lifetimes. However, from Figs. 5 and 6 we can make qualitative judgements based on prompt versus delayed fluorescence signals.

Polarization sensitivity is the hallmark of electron recollision. If the fluorescence measured here vanished for circularly polarized pulses, we would identify recollision as the excitation process. We therefore show the circular/linear signal ratios for various nitrogen and argon lines in Fig. 7.

### IV. DISCUSSION

#### A. Observations

Figure 8 summarizes the pressure dependence of all argon and nitrogen fluorescence lines. Based on this figure, we

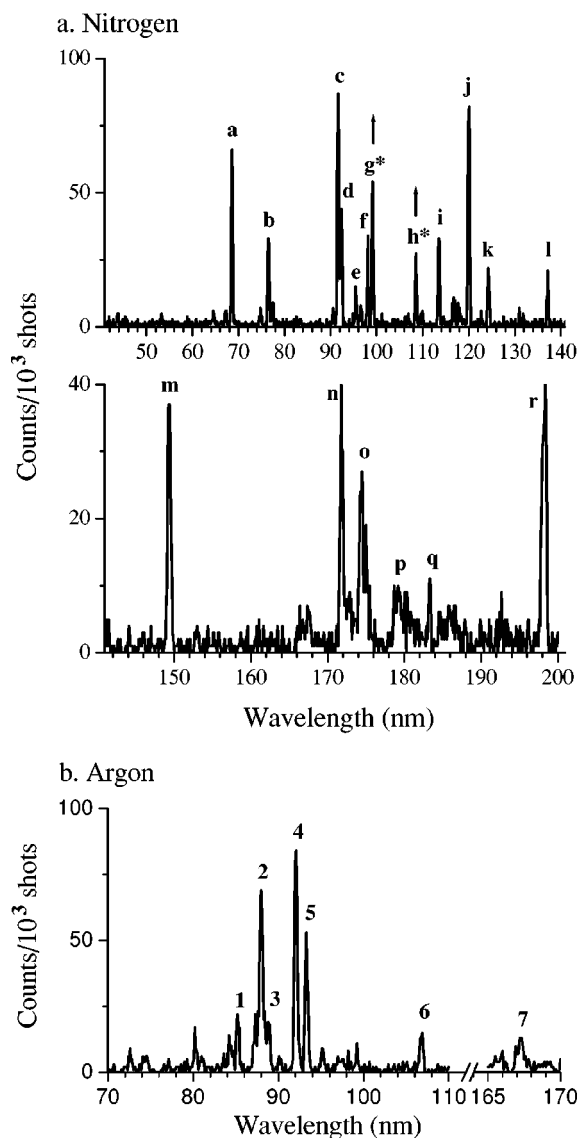


FIG. 3. (a) vuv spectrum of  $N_2$  from 40–200 nm. (b) vuv spectrum of Ar from 70–110 nm and 165–170 nm. Spectra are obtained with 0.1 nm steps and accumulating  $10^3$  laser shots per step. A pressure of 100 mtorr was used and the laser intensity was  $\sim 10^{14}$  W/cm<sup>2</sup>. Note \* denotes that the corresponding peak is shown reduced by a factor of 10.

clearly distinguish two groups of lines; one group has a power law  $m$  near 1.0 and another near 1.7. Our endeavor now is to identify each group with a different excitation mechanism. Plasma excitation is an inherently many-body process whose complicated nature makes a detailed characterization difficult. Attempting to avoid such complication, we simply attribute lines with  $m > 1.4$  to plasma excitation. All of the argon lines and eight of the nitrogen lines lie above  $m = 1.4$  and are therefore ascribed to plasma excitation. Direct laser excitation involves only one particle interacting with the laser field and therefore must have a linear pressure dependence. Ten nitrogen lines, including two unidentified transitions, lie below  $m = 1.4$ . From this we conclude that these transitions are produced by direct laser excitation.

TABLE I. Fluorescence details and excitation summary.

Label	Species	Configuration	Excitation	Timing <sup>a</sup>	Process
<i>a</i>	N <sup>2+</sup>	$2s^2(1S)2p^2P^o [0 \text{ eV}] \leftarrow 2s2p^2^2P [18.1 \text{ eV}]$	$2s^{-1}$	Prompt	Laser
<i>b</i>	N <sup>2+</sup>	$2s^2(1S)2p^2P^o [0 \text{ eV}] \leftarrow 2s2p^2^2S [16.2 \text{ eV}]$	$2s^{-1}$		Laser
	N <sup>3+</sup>	$2s^2^1S [0 \text{ eV}] \leftarrow 2s(2S)2p^1P^o [16.2 \text{ eV}]$	$2s^{-1}$		
<i>c</i>	N <sup>+</sup>	$2s^2(1S)2p2^3P [0 \text{ eV}] \leftarrow 2s(2S)2p^3P^o [13.5 \text{ eV}]$	$2s^{-1}$	Delayed fall	Plasma
<i>d</i>	N <sup>3+</sup>	$2s(2S)2p^3P^o [8.3 \text{ eV}] \leftarrow 2p^2^3P [21.8 \text{ eV}]$	$2s^{-2}$	Prompt	Laser
<i>e</i>	N	$2s^22p^3^4S^o [0 \text{ eV}] \leftarrow 2s^22p^2(3P)3d^4P [13.0 \text{ eV}]$	Rydberg		Plasma
<i>f</i>	N <sup>2+</sup>	$2s2p^2^2D [12.5 \text{ eV}] \leftarrow 2p^3^2D^o [25.2 \text{ eV}]$	$2s^{-2}$		Laser
<i>g</i>	N <sup>2+</sup>	$2s^2(1S)2p^2P^o [0 \text{ eV}] \leftarrow 2s2p^2^2D [12.5 \text{ eV}]$	$2s^{-1}$	Prompt	Laser
<i>h</i>	N <sup>+</sup>	$2s^2(1S)2p^2^3P [0 \text{ eV}] \leftarrow 2s(2S)2p^3^3D^o [11.4 \text{ eV}]$	$2s^{-1}$	Prompt	Laser
<i>i</i>	N	$2s^22p^3^4S^o [0 \text{ eV}] \leftarrow 2s2p^4P [10.9 \text{ eV}]$	$2s^{-1}$	Delayed	Plasma
<i>j</i>	N	$2s^22p^3^4S^o [0 \text{ eV}] \leftarrow 2s^22p^2(3P)3s^4P [10.3 \text{ eV}]$	Rydberg	Delayed fall	Plasma
<i>k</i>	N	$2s^22p^3^2D^o [2.4 \text{ eV}] \leftarrow 2s^22p^2(1D)3s^2D [12.4 \text{ eV}]$	Rydberg		Plasma
<i>l</i>		Unidentified			Laser
<i>m</i>	N	$2s^22p^3^2D^o [2.4 \text{ eV}] \leftarrow 2s^22p^2(3P)3s^2P [10.7 \text{ eV}]$	Rydberg	Delayed	Plasma
<i>n</i>	N <sup>3+</sup>	$2s(2S)2p^1P^o [16.2 \text{ eV}] \leftarrow 2p^2^1D [23.4 \text{ eV}]$	$2s^{-2}$		Laser
<i>o</i>	N	$2s^22p^3^2P^o [3.6 \text{ eV}] \leftarrow 2s^22p^2(3P)3s^2P [10.7 \text{ eV}]$	Rydberg	Delayed	Plasma
<i>p</i>		Unidentified			Laser
<i>q</i>		Unidentified			Plasma
<i>r</i>	N <sub>2</sub> <sup>+</sup>	$X^2\Sigma_g^+ \leftarrow C^2\Sigma_u^+$			Laser
1	Ar <sup>3+</sup>	$3s^23p^3^4S^o [0 \text{ eV}] \leftarrow 3s3p^4^4P [14.6 \text{ eV}]$	$3s^{-1}$		Plasma
2	Ar	$3s^23p^6^1S [0 \text{ eV}] \leftarrow 3s^23p^5(2P^o_{3/2})5s^2[3/2]^o [14.1 \text{ eV}]$	Rydberg	Prompt	Plasma <sup>b,c</sup>
	Ar <sup>2+</sup>	$3s^23p^4^3P [0.1 \text{ eV}] \leftarrow 3s3p^5^3P^o [14.2 \text{ eV}]$	$3s^{-1}$		
3	Ar <sup>2+</sup>	$3s^23p^4^3P [0.1 \text{ eV}] \leftarrow 3s3p^5^3P^o [14.1 \text{ eV}]$	$3s^{-1}$		Plasma
4	Ar <sup>+</sup>	$3s^23p^5^2P^o [0 \text{ eV}] \leftarrow 3s3p^6^2S [13.5 \text{ eV}]$	$3s^{-1}$	Prompt	Plasma
5	Ar <sup>+</sup>	$3s^23p^5^2P^o [0.2 \text{ eV}] \leftarrow 3s3p^6^2S [13.5 \text{ eV}]$	$3s^{-1}$		Plasma
6	Ar	$3s^23p^6^1S [0 \text{ eV}] \leftarrow 3s^23p^5(2P^o_{3/2})4s^2[3/2]^o [11.6 \text{ eV}]$	Rydberg	Delayed	Plasma <sup>c</sup>
7	Ar <sup>2+</sup>	$3s^23p^3(4S^*)3d^5D [18.0 \text{ eV}]$ $\leftarrow 3s^23p^3(4S^*)4p^5P [25.4 \text{ eV}]$	Rydberg		Plasma

<sup>a</sup>These judgements are qualitatively based on figures similar to Figs. 5 and 6 and serve only to confirm identifications based on pressure dependence; a prompt signal is necessary, but not sufficient, for direct excitation.

<sup>b</sup>A transition very near this line has been produced via laser-induced resonance [28].

<sup>c</sup>Observed via laser-induced  $e^-$  rescattering [31].

In addition, direct laser excitation can only produce excited population during the pulse. Our fluorescence signals will then decay at the well-known rates,  $A_{ij}$  [27]. The decay rates for all of the lines shown in Fig. 5 and 6 are faster than our detector response to a vuv impulse,  $t_{f,115} = 12.3$  ns; therefore, direct fluorescence must closely track this impulse response. For example, Fig. 5(a) shows that nitrogen peak *g* follows the vuv impulse response almost perfectly, and indeed peak *g* has a linear pressure dependence [Fig. 8(b)]. Furthermore, any delayed fluorescence [Figs. 5(b), 5(c), and 6(b)] must belong to the group of lines with *m* near 1.7 in Fig. 8, as indeed they do. Clearly the timing of a fluorescence signal provides confirmation that a transition with a linear pressure dependence should be ascribed to direct laser excitation. In Table I, one can see that all signals associated with direct laser excitation that were measured for timing are prompt. All delayed signals are associated with plasma excitation, but not the reverse. For instance, the argon peak 4 appears prompt in Fig. 6(a), but its pressure dependence indicates

that it is a plasma-induced transition. This reminds us that a prompt signal is necessary, but not sufficient, for identification with direct excitation; a plasma process might very well be fast, but it will never have a linear pressure dependence.

Recalling the symbol convention mentioned above, Fig. 8 shows a correlation between excitation mechanism and excitation type. Direct laser excitation occurs only in nitrogen and it produces exclusively  $2s^{-1(2)}$  fragment excitations, along with one molecular and two unidentified excitations. In the light of these identifications, we now compare the three models mentioned above; laser-induced resonance, laser-induced  $e^-$  rescattering, and enhanced multiphoton susceptibility in diatomic molecules.

### B. Direct laser excitation

Prior to the recent work of Refs. [14,15], the most likely candidate for direct multiphoton excitation would have been population transfer via laser-induced resonance. First appear-

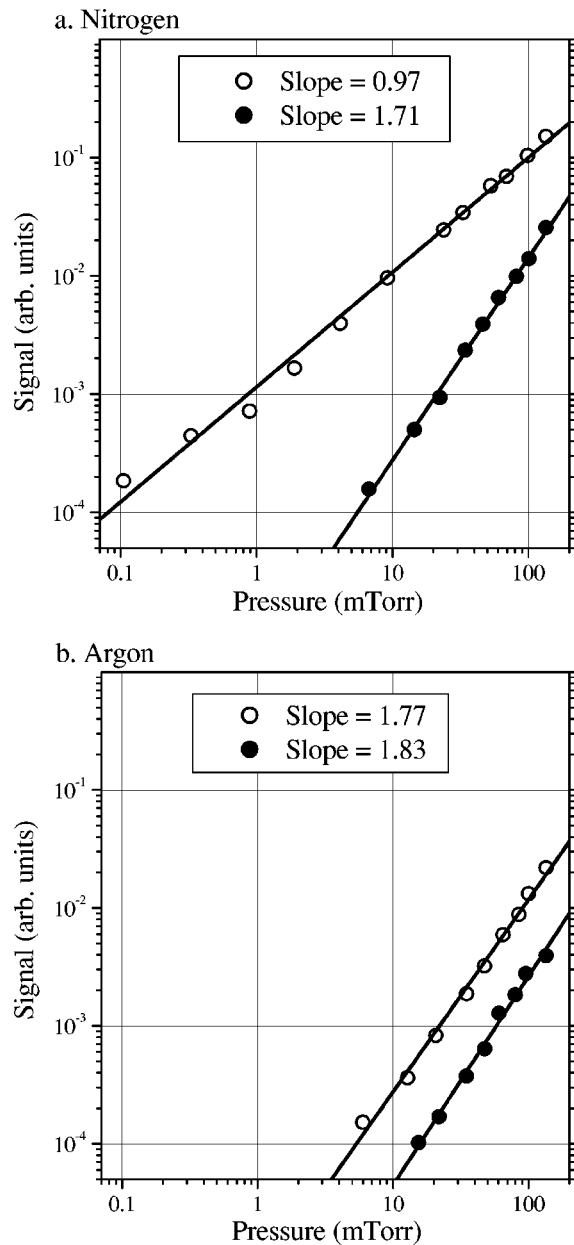


FIG. 4. (a) (○) Pressure dependence of the  $N^{2+}$  inner-valence transition peak *g* and (●) the Rydberg N transition peak *j*. (b) (○)  $Ar^+$  inner-valence transition peak 4 and (●) Ar Rydberg transition peak 6. Photon counts are integrated over a 200 ns range for each data point. Also plotted are the linear fits whose slopes distinguish plasma and direct signals as described in the text.

ing as Rydberg series in photoelectron spectra [12,16,28], excited states are ac Stark shifted into multiphoton resonance where they enhance ionization [29]. In addition to ionization, a small population ( $\sim 1\%$ ) could remain in those excited states [17,30]. Since many different states ac Stark shift into resonance, it is hard to imagine that there could be any selectivity for such an excitation. In fact, since the excitations lie near the ionization limit, one would expect to see primarily Rydberg excitations. Indeed the  $4f$ ,  $5f$ ,  $6f$ ,  $4s$ , and  $4s'$  levels of argon are the states that aid intense laser ionization [29,30]. Beyond photoelectron spectra, laser-induced reso-

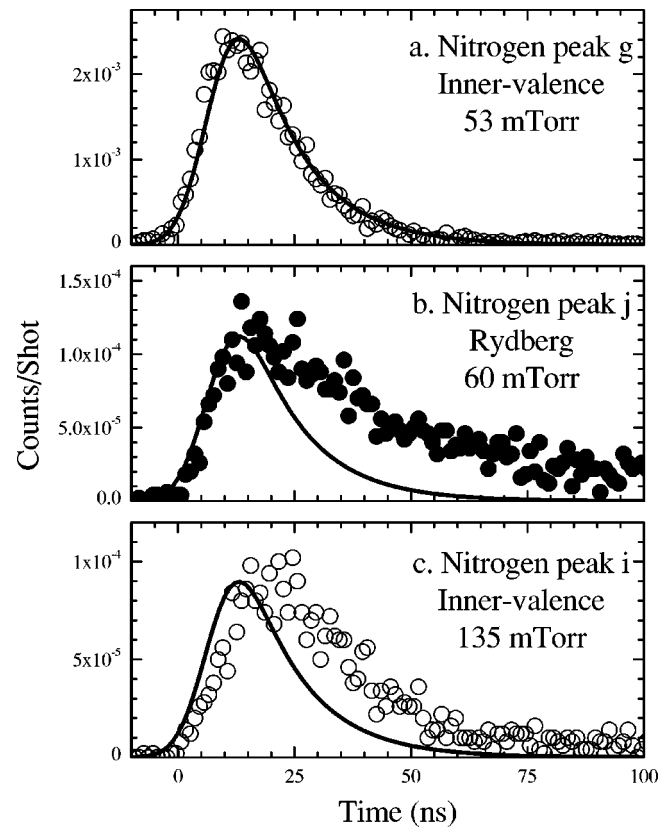


FIG. 5. (a) (○) The timing signal for an  $N^{2+}$  inner-valence transition closely follows the impulse response. (b) (●) A  $N^{0+}$  Rydberg transition clearly exhibits a delayed signal fall time. (c) (○) An inner-valence  $N^{0+}$  transition also exhibits a delayed fall time. All three transition lifetimes 2.0, 2.5, and 6.5 ns, respectively, are shorter than the system response (included as the solid line). Clearly, delayed signal fall times are not due to their natural transition rates,  $1/A_{ij}$ .

nance does in fact produce  $3p \leftarrow 3d$  vuv fluorescence in argon [28]. Plasma excitation accounts for all argon fluorescence in our data, suggesting that excitation from laser-induced resonance lies below our detection threshold. Our strongest directly excited peak is over three orders of magnitude above that threshold.

Another possible explanation is inelastic electron rescattering [13]. An electron lost in ionization can be accelerated by the light field to return and collide with the parent molecule. Excitation and subsequent fluorescence from such a process would not only exhibit a linear pressure dependence, but also it would exhibit prompt timing. However, highly dependent on impact parameter, rescattering cannot occur for circularly polarized pulses [18]. Yet, we see in Fig. 7 that all fluorescence lines tested remain for circular polarization. In fact, direct signals decrease only by about a factor of 2, nowhere near the “turn off” predicted by the rescattering scheme. Furthermore,  $e^-$  scattering excitations are indiscriminate while the excitations in our experiment are highly selective [9]. Finally, laser-induced  $e^-$  rescattering causes argon to fluoresce at peaks 2 and 6 [31], but as noted before, these peaks are produced by plasma excitation in our experiment. Like laser-induced resonance,  $e^-$  rescattering occurs

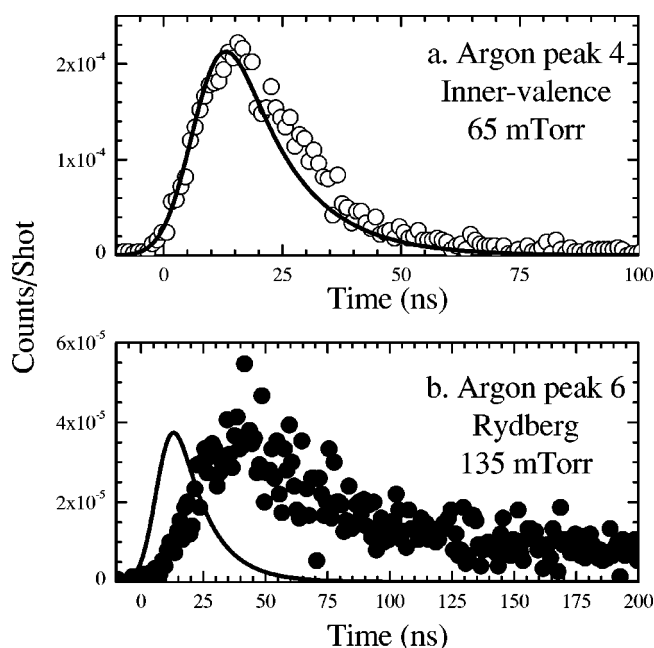


FIG. 6. (a) (○)  $\text{Ar}^+$  inner-valence transition with a lifetime of 7.1 ns. (b) (●) Neutral Ar Rydberg transition with a lifetime of 8.4 ns. Note the different time scales show that the Rydberg transition is significantly delayed.

below our detection threshold. The direct fluorescence reported here must have another explanation.

Still, one might think of exciting a manifold of transient molecular states that somehow funnel into specific dissociative channels. In fact, the familiar excimer system uses a plasma discharge to produce a statistical distribution of excited states. This manifold then “cools” into the long-range molecular state for the lasing transition. However, the NIST tables [27,32] and our own data confirm that plasma excitations lead to both inner-valence and Rydberg excitations.

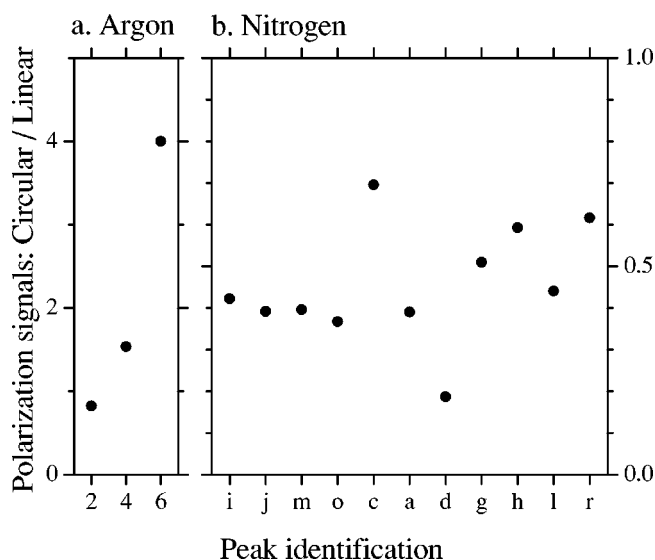


FIG. 7. Ratio of the signal for circular vs linear polarization. The signals were measured at a laser intensity of  $\sim 10^{14}$  W/cm<sup>2</sup> and a pressure of 100 mtorr.

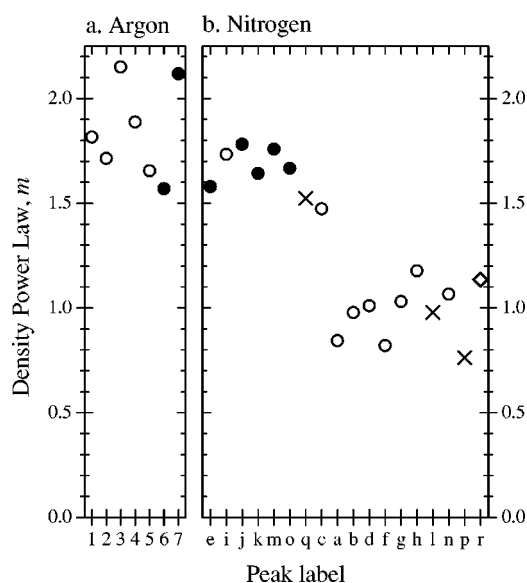


FIG. 8. Density power law, measured by the slope of the density dependence as described in the text. Peak labels correspond to those used in Fig. 3. (●) Rydberg excitation, (○) inner-valence excitation, (◇)  $\text{N}_2^+ : X \leftarrow B$  transition, and (×) unidentified excitation.

Furthermore, inelastic  $e^-$  scattering leads to both types of fluorescence states [9]. Synchrotron photodissociation and dissociative ionization similarly reveal both inner-valence and Rydberg excited fragments [10]. If there were some mechanism for transferring indiscriminate excitation into just one specific type of excited state, the past work with  $\text{N}_2$  certainly would have uncovered it.

Our predominance of highly charged  $2s^{-1(2)}$  excited fragments clearly shows that ultrashort pulse ionization favors channels that leave fragments stripped of one or more inner-valence electrons. The  $2s$  atomic orbital correlates to the  $2\sigma_g$  and  $2\sigma_u$  molecular orbitals, which form a charge-transfer pair that has attracted quite some interest. The  $2\sigma_g^{-1}$  excitation was cited in asymmetric x-ray Auger decay [11] and again in ultrafast laser-induced charge-asymmetric dissociation [2]. Subpicosecond 248 nm pulses led to the observation of a novel  $2\sigma_g^{-1}$  molecular excitation with a 55.8 nm fluorescence line [6]. Ultrashort pulses also produce fluorescence from the  $\text{N}_2^+ : B(2\Sigma_u^+)$  state which primarily consists of the  $2\sigma_u^{-1}$  excitation [22,34]. A mechanism by which intense laser pulses couple to charge-transfer states could explain not only the predominance of asymmetric dissociation, but also the selective fluorescence from ultrafast multiphoton ionization [3,4,35,36].

The ground state and a charge-transfer pair together give a three-level structure that reveals a unique multiphoton coupling scheme. Unlike laser-induced resonance, this coupling scheme maintains a field-free resonance throughout the pulse [14,15]. The theory predicts that a pair of nearly degenerate charge-transfer states can interact with a strong light field to create a Floquet ladder. In homonuclear molecules this interaction introduces *no* ac Stark shift. It then takes just a single photon to couple a rung of the Floquet ladder to the ground state. The only ac Stark shift is due to this much weaker single-photon coupling, allowing a field-free multiphoton

resonance throughout the duration of the pulse. This system is highly selective since it couples the ground state to one pair of excited states. It therefore predicts the efficient and selective excitation of evenly charged diatomic molecules.

The observation of charge-asymmetric dissociation implies that charge transfer to symmetric channels would involve fragment excitation;  $(N_2^{2+})^* \rightarrow N + N^{2+} \rightarrow N^+ + (N^+)^*$  [3]. In fact, asymmetric channels can even lead to excited fragments without transferring to a symmetric channel;  $(N_2^{2+})^* \rightarrow (N^{2+})^* + N$  [4,5]. Likewise, even more highly charged molecules that exhibit prominent asymmetric channels could lead to multiply ionized excited fragments. Since our direct excitations are primarily highly charged  $2s^{-1(2)}$  excited fragments and since the  $2\sigma_{g,u}$  states map to the  $2s$  in the separated atom limit [23,37], our results indeed suggest that charge-transfer molecular states are responsible for the exclusivity of fragment excitations observed here. Thus, our results appear to support the recently proposed three-level multiphoton coupling scheme [14,15].

## V. CONCLUSION

By distinguishing fluorescence lines resulting from plasma and direct excitation, we demonstrate selective excitation imparted to the highly charged fragments of multiphoton dissociative ionization. Ten of the 18 nitrogen fluorescence lines display a linear density dependence indicating direct laser excitation. Persistence with circular polarization confirms that these fluorescence lines must result from an excitation mechanism of the parent molecule other than electron rescattering. Furthermore, this direct laser excitation exclusively produces inner-valence excitations in the dissociative fragments. Such selectivity rules out the inherently indiscriminate laser-induced resonance. The high selectivity

for  $2s^{-1(2)}$  fragment states is far better explained by a recent theory regarding the  $\sigma_u\text{-}\sigma_g$  charge-transfer states of even-charged diatomic molecules [14,15]. Indeed we are observing a highly selective excitation mechanism in the extreme multiphoton coupling regime.

Efficient and selective population transfer has important consequences for future research with ultrashort pulsed lasers. The most obvious application is the production of population inversions for the amplification of attosecond lasers [38–40]. One needs only a very short inversion window to amplify the seed pulse. Since the inversion would occur in strongly dissociative potential curves one could think of pulse shaping and evolutionary algorithms to “focus” the nuclear wave function at some optimal internuclear separation [41]. Such an inversion could be optimized so that it is momentarily resonant with an attosecond seed pulse. In fact, such a system might be implemented for any high-harmonic amplification.

Another intriguing route could be the extreme multiphoton analog to  $\omega\text{-}3\omega$  excitation-path interference [42–44]. Through frequency doubling, the interference of  $2\omega\text{-}4\omega$  processes might alter dissociation channel branching ratios. One could also test the nature of the degeneracy between strongly coupled gerade and ungerade states by looking for interference effects between even-odd photon processes such as a  $3\omega\text{-}6\omega$  pathway interference. Ultimately, excitation selectivity from ultrashort pulses will lead to a better understanding of molecular dynamics and it could open a new realm of laser science in the multiphoton regime.

## ACKNOWLEDGMENTS

We would like to thank P. B. Corkum for insightful conversation. We also acknowledge our support from the NSF under Grant No. NSF-PHYS-9987804.

- 
- [1] D. T. Strickland, Y. Beaudoin, P. Dietrich, and P. B. Corkum, *Phys. Rev. Lett.* **68**, 2755 (1992).
  - [2] K. Boyer, T. S. Luk, J. C. Solem, and C. K. Rhodes, *Phys. Rev. A* **39**, 1186 (1989).
  - [3] G. N. Gibson, M. Li, C. Guo, and J. P. Nibarger, *Phys. Rev. A* **58**, 4723 (1998).
  - [4] C. Guo, M. Li, and G. N. Gibson, *Phys. Rev. Lett.* **82**, 2492 (1999).
  - [5] J. P. Nibarger, M. Li, S. Menon, and G. N. Gibson, *Phys. Rev. Lett.* **83**, 4975 (1999).
  - [6] G. Gibson, T. S. Luk, A. McPherson, K. Boyer, and C. K. Rhodes, *Phys. Rev. A* **40**, 2378 (1989).
  - [7] L. Quaglia and C. Cornaggia, *Phys. Rev. Lett.* **84**, 4565 (2000).
  - [8] A. Lofthus and P. H. Krupenie, *J. Phys. Chem. Ref. Data* **6**, 235 (1977).
  - [9] J. M. Ajello, G. K. James, B. O. Franklin, and D. E. Sheman-sky, *Phys. Rev. A* **40**, 3524 (1989).
  - [10] L. C. Lee, R. W. Carlson, D. L. Judge, and M. Ogawa, *J. Chem. Phys.* **61**, 3261 (1991).
  - [11] W. Eberhardt, E. W. Plummer, I.-W. Lyo, R. Carr, and W. K. Ford, *Phys. Rev. Lett.* **58**, 207 (1987).
  - [12] R. R. Freeman and P. H. Bucksbaum, *J. Phys. B* **24**, 325 (1991).
  - [13] P. B. Corkum, *Phys. Rev. Lett.* **71**, 1994 (1993).
  - [14] G. N. Gibson, *Phys. Rev. Lett.* **89**, 263001 (2002).
  - [15] G. N. Gibson, *Phys. Rev. A* **67**, 043401 (2003).
  - [16] R. R. Freeman, P. H. Bucksbaum, H. Milchberg, S. Darack, D. Schumacher, and M. E. Geusic, *Phys. Rev. Lett.* **59**, 1092 (1987).
  - [17] R. R. Jones, D. W. Schumacher, and P. H. Bucksbaum, *Phys. Rev. A* **47**, R49 (1993).
  - [18] H. Nii-kura, F. Légaré, R. Hasbani, A. D. Bandrauk, M. Y. Ivanov, D. M. Villeneuve, and P. B. Corkum, *Nature (London)* **417**, 917 (2002).
  - [19] P. Dietrich, N. H. Burnett, M. Ivanov, and P. B. Corkum, *Phys. Rev. A* **50**, R3585 (1994).
  - [20] V. R. Bhardwaj, D. M. Rayner, D. M. Villeneuve, and P. B. Corkum, *Phys. Rev. Lett.* **87**, 253003 (2001).
  - [21] R. S. Mulliken, *J. Chem. Phys.* **7**, 20 (1939).
  - [22] A. Becker, A. D. Bandrauk, and S. L. Chin, *Chem. Phys. Lett.* **343**, 345 (2001).

- [23] G. Herzberg, *The Spectra and Structures of Simple Free Radicals: An Introduction to Molecular Spectroscopy* (Cornell University Press, Ithaca, NY, 1971).
- [24] M. Li and G. N. Gibson, *J. Opt. Soc. Am. B* **15**, 2404 (1998).
- [25] Acton Research Corporation, <http://www.acton-research.com/>
- [26] McPherson, Inc. <http://mcphersoninc.com/detectors/model650detectorassembly>
- [27] Physics Laboratory at the National Institute of Standards and Technology (NIST), [http://physics.nist.gov/cgi-bin/AtData/main\\_asd](http://physics.nist.gov/cgi-bin/AtData/main_asd)
- [28] M. P. Hertlein, P. H. Bucksbaum, and H. G. Muller, *J. Phys. B* **30**, L197 (1997).
- [29] G. N. Gibson, R. R. Freeman, and T. J. McIlrath, *Phys. Rev. Lett.* **69**, 1904 (1992).
- [30] M. P. de Boer and H. G. Muller, *Phys. Rev. Lett.* **68**, 2747 (1992).
- [31] A. Becker, F. H. M. Faisal, Y. Liang, S. Augst, Y. Beaudoin, M. Chaker, and S. L. Chin, *J. Phys. B* **33**, L547 (2000).
- [32] *CRC Handbook of Chemistry and Physics*, edited by J. Reader and C. H. Corliss, 19th ed. (CRC Press, Boca Raton, FL, 1998), also published as Ref. [33].
- [33] J. Reader, C. H. Corliss, W. L. Wiese, and G. A. Martin, *Wavelengths and Transition Probabilities for Atoms and Atomic Ions* (National Bureau of Standards, Washington, D.C., 1980), Vol. 68.
- [34] A. Talebpour, A. Bandrauk, and S. L. Chin, in *Multiphoton Processes*, edited by Louis F. DiMauro, Richard R. Freeman, and Kenneth Kulander, AIP Conf. Proc. No. 525 (AIP, Melville, NY, 2000), pp. 508–516.
- [35] J. P. Nibarger, S. V. Menon, and G. N. Gibson, *Phys. Rev. A* **63**, 053406 (2001).
- [36] S. V. Menon, J. P. Nibarger, and G. N. Gibson, *J. Phys. B* **35**, 2961 (2002).
- [37] A. D. Bandrauk, D. G. Musaev, and K. Morokuma, *Phys. Rev. A* **59**, 4309 (1999).
- [38] A. Paul, R. A. Bartels, R. Tobey, H. Green, S. Weiman, I. P. Christov, M. M. Murnane, H. C. Kapteyn, and S. Backus, *Nature (London)* **421**, 51 (2003).
- [39] P. M. Paul, E. S. Toma, P. Berger, G. Mullot, F. Augé, P. Balcou, H. G. Muller, and P. Agostini, *Science* **292**, 1689 (2001).
- [40] M. Drescher, M. Hentschel, R. Keinberger, G. Tempea, C. Spielmann, G. A. Reider, P. B. Corkum, and F. Krausz, *Science* **291**, 1923 (2001).
- [41] R. Sauerbrey and B. R. Johnson, *Opt. Lett.* **19**, 64 (1994).
- [42] C. Chen, Y.-Y. Yin, and D. S. Elliott, *Phys. Rev. Lett.* **64**, 507 (1990).
- [43] C. Chen and D. S. Elliott, *Phys. Rev. Lett.* **65**, 1737 (1990).
- [44] L. Zhu, V. Kleiman, X. Li, S. P. Lu, K. Trentelman, and R. J. Gordon, *Science* **270**, 77 (1995).